Quantized linear σ model at finite temperature, and nucleon properties

M. Abu-Shady
Department of Mathematics, Faculty of Science, Menofiya University, Egypt

H. M. Mansour
Department of Physics, Faculty of Science, Cairo University, Egypt

(Received 11 October 2011; revised manuscript received 12 January 2012; published 17 May 2012)

The nucleon properties due to the restoration of the chiral symmetry at nonzero temperature T are investigated within the framework of the linear σ model. The field equations are solved using the coherent-pair approximation. In this approach, the quantum fields are treated in a nonperturbative fashion. We minimize the expectation value of the chiral Hamiltonian using the ansatz of the coherent-pair ground-state configuration. The obtained results show that the nucleon mass and mean-square radius of the proton and the neutron increase monotonically with the temperature T and that the pion-nucleon coupling constant $g_{\pi NN}$ decreases with temperature values that are near the value of the critical temperature T_c. The nucleon mass and mean-square radius of the proton are examined in the (x, T) plane, showing a sensitive dependence on the coherence parameter x. This means that an increase of both the coherence parameter x and the temperature T leads to an increase in the values of the nucleon mass and the mean-square radius of the proton. This is evidence for the quark-gluon deconfinement phase transition.

DOI: 10.1103/PhysRevC.85.055204 PACS number(s): 14.20.Dh, 11.30.Rd, 12.38.Aw, 12.38.Mh

I. INTRODUCTION

In recent years, the behavior of strongly interacting matter under extreme conditions of temperature has become an issue of great interest because of its relevance to particle physics and astrophysics. In particular, it is important to study how hadron properties (masses, magnetic moments, decay constants, etc.) can be modified when hadrons propagate in a hot medium [1]. The study of hadron properties at finite temperature and density is essential for understanding the behavior of quarks and gluons in the hot QCD medium, which is called quark gluon plasma (QGP). This phase is under investigation in RHIC [2], BNL, and CERN experiments [3] and there is strong evidence that it has been observed. The low critical values of the temperature mean that one has to deal with nonperturbative phenomena. However, the analytical as well as the numerical (lattice QCD) methods have not been developed enough to fully allow for the solution of low-energy nonperturbative cases, especially if the baryons are involved. Therefore one may apply effective quark models, which satisfy chiral symmetry and spontaneous symmetry breaking.

Chiral symmetry breaking is an important phenomenon in hadron physics and is of fundamental importance for hadron properties. The difficulties involved in obtaining low-energy properties directly from QCD, the fundamental theory of strong interactions, have motivated the construction of effective models due to their simplicity and effectiveness in describing hadrons at low energies [4]. The linear σ model has been proposed as a model for strong nuclear interactions [5]. The model was first proposed as a model for pion-nucleon interactions. Today it serves as an effective model for the low-energy phase (zero temperature) of quantum chromodynamics [6–9] and its modification is suggested as in Refs. [10–15] to provide a good description of the baryon properties. The model exhibits the spontaneous breaking of chiral symmetry and its restoration at finite temperatures. This model has been extensively studied recently [16–22]. The Hartree approximation of the $O(N)$ linear σ model of two or four quarks flavors has been studied at finite temperature by various authors [16,19–21]. The model with spontaneous symmetry breaking is found to have a first-order phase transition towards the symmetric phase at high temperatures. In contrast to the case of large N, the mass of the pion quantum fluctuations does not vanish in the broken phase [16–18,22]. The order of phase transitions depends on the loops, which are taken into account in the effective potential [23]. Moreover, the isospin chemical potential is investigated in this model using the Cornwall-Jackiw-Tombolis (CJT) formalism [24] as in Refs. [25–27]. Lenaghan and Rischke [28] used the CJT formalism to study the σ and pion masses and obtained the meson masses at a given nonzero temperature, which generally depends on the choice of the cutoff or renormalization. Chiku and Hatsuda [29] applied the optimized perturbation theory at finite temperature T in the linear σ model and the higher-order terms are considered in their approach.

The quark σ model is successfully applied to the description of static and dynamic baryon properties at finite temperature and density as in Refs. [30,31]. The description is in quantitative agreement in comparison with other approaches. On the same lines, Dominguez *et al*. [32] studied the behaviors of the pion-nucleon coupling constant and the mean-square radius of the nucleon as functions of the temperature in the framework of the thermal σ model and the thermal QCD finite energy sum rules without considering the quantization of the fields. Zakout [33] introduced another approach to investigate the nucleon mass at finite temperature using the Bethe-Salpeter equation (BSE) and compared his results with those of the MIT bag model. Caldas *et al*. [34] studied the linear σ model at finite temperature, in which a modified self-consistent resummation (MSCR) was applied.

The aim of this work is to investigate the nucleon properties in the framework of the linear σ model at finite temperature

considering the quantization of fields. In Refs. [8,9], the nucleon properties are calculated at zero temperature, taking the quantized fields into account. Many recent works have not considered the quantization of the fields at finite temperatures [19].

In Sec. II, the quark σ model with the effective mesonic potential is explained. The Fock state in the coherent-pair approximation and the variational principle are presented in Secs. III and IV, respectively. The derived nucleon properties are calculated at finite temperature in Sec. V. The numerical calculations and the results are presented in Sec. VI. We discuss and summarize the results in Sec. VII.

II. QUARK σ MODEL WITH EFFECTIVE MESONIC POTENTIAL

The Lagrangian density of the quark σ model that describes the interactions between quarks via the σ and π mesons with the effective mesonic potential of one loop takes the following form [35]

$$L(r) = i\overline{\Psi}\partial_\mu\gamma^\mu\hat{\Psi} + \tfrac{1}{2}(\partial_\mu\hat{\sigma}\,\partial^\mu\hat{\sigma} + \partial_\mu\hat{\pi}\cdot\partial^\mu\hat{\pi}) + g\hat{\overline{\Psi}}(\hat{\sigma} + i\gamma_5\hat{\tau}\cdot\hat{\pi})\hat{\Psi} - U^{\text{eff}}(\hat{\sigma},\hat{\pi}), \tag{1}$$

with

$$U^{\text{eff}}(\hat{\sigma},\hat{\pi}) = \frac{\lambda^2}{4}(\hat{\sigma}^2+\hat{\pi}^2-\nu^2)^2 - f_\pi m_\pi^2\hat{\sigma} - \frac{\pi^2}{45}T^4 + \frac{T^2}{24f_\pi^2}\left(3m_\sigma^2-5m_\pi^2\right)(\hat{\sigma}^2+\hat{\pi}^2), \tag{2}$$

where

$$\lambda^2 = \frac{m_\sigma^2-m_\pi^2}{2f_\pi^2}, \quad \nu^2 = f_\pi^2 - \frac{m_\pi^2}{\lambda^2}, \tag{3}$$

where f_π is the pion decay constant, m_π is the pion mass, and m_σ and g are constants to be determined. The quark, σ, and π mesons are quantum fields denoted by $\hat{}$. In Eq. (2), the first and second terms on the right side represent a contribution from the meson at the tree level of the usual mesonic potential with explicit symmetry breaking term at zero temperature. The third term arises from the quark loop, and the final term is from the meson loop (for details, see Ref. [35])

Now one can rewrite the Hamiltonian density [9]

$$\hat{H}(r) = \tfrac{1}{2}\{\hat{P}_\sigma(r)^2 + [\nabla\hat{\sigma}(r)]^2 + \hat{P}_\pi(r)^2 + [\nabla\pi(r)]^2\} + U^{\text{eff}}(\hat{\sigma},\hat{\pi}) + \hat{\Psi}^\dagger(r)(-i\alpha\nabla)\hat{\Psi}(r) - g(r)\,\hat{\Psi}^\dagger(r)[\beta\hat{\sigma}(r) + i\beta\gamma_5\hat{\tau}\cdot\hat{\pi}]\hat{\Psi}(r), \tag{4}$$

where α and β are the usual Dirac matrices. In the above expression, $\hat{\overline{\Psi}}$, $\hat{\sigma}$ and $\hat{\pi}$ are quantized field operators with the appropriate static angular momentum expansion [8, 9],

$$\hat{\sigma}(r) = \int_0^\infty \frac{dkk^2}{[2(2\pi)^3 W_\sigma(k)]^{\frac{1}{2}}}[\hat{c}^\dagger(k)\,e^{-ik.r} + \hat{c}(k)\,e^{+ik.r}], \tag{5}$$

$$\hat{\pi}(r) = \left[\frac{2}{\pi}\right]^{\frac{1}{2}}\int_0^\infty dkk^2\left[\frac{1}{2W_\pi(k)}\right]^{\frac{1}{2}}\sum_{lmw} j_l(kr)\,Y_{lm}^*(\Omega_r) \times\left[\hat{a}_{lm}^{1w\dagger}(k) + (-)^{m+w}\,\hat{a}_{l-m}^{1-w}(k)\right], \tag{6}$$

$$\hat{\Psi}(r) = \sum_{njmw}\left(\langle r\uparrow njmw\rangle\,\hat{d}_{njm}^{\frac{1}{2}w} + \langle r\uparrow\overline{n}jmw\rangle\,\hat{d}_{njm}^{\frac{1}{2}w\dagger}\right), \tag{7}$$

where the $|njmw\rangle$ and $|\overline{n}jmw\rangle$ form a complete set of quark and antiquark spinors with angular momentum quantum numbers and spin-isospin quantum numbers j, m, and w, respectively. The corresponding conjugate momentum fields have the expansion [8,9],

$$\hat{P}_\sigma(r) = i\int_0^\infty dkk^2\left[\frac{W_\sigma(k)}{2(2\pi)^3}\right]^{\frac{1}{2}}[\hat{c}^\dagger(k)\,e^{-\mathbf{k}.\mathbf{r}} - \hat{c}(k)\,e^{+\mathbf{k}.\mathbf{r}}], \tag{8}$$

$$\hat{P}_\pi(r) = i\left[\frac{2}{\pi}\right]^{\frac{1}{2}}\int_0^\infty dkk^2\left[\frac{W_\pi(k)}{2}\right]^{\frac{1}{2}}\sum_{lmw} j_l(kr)\,Y_{lm}^*(\Omega_r) \times\left[\hat{a}_{lm}^{1w\dagger}(k) - (-)^{m+w}\,\hat{a}_{l-m}^{1-w}(k)\right]. \tag{9}$$

Here $\hat{c}(k)$ destroys a σ quantum with momentum $\mathbf{k}$ and frequency $W_\sigma(k) = (k^2+m_\sigma^2)^{\frac{1}{2}}$ and $\hat{a}_{lm}^{1w}(k)$ destroys a pion with momentum $\mathbf{k}$ and corresponding frequency $W_\pi(k) = (k^2+m_\pi^2)^{\frac{1}{2}}$ in the isospin-angular momentum state $\{lm;tw\}$.

III. FOCK STATE

For convenience, one constructs the configuration-space pion field functions, which are needed for the subsequent variational treatment by defining the alternative basis operators,

$$\hat{b}_{lm}^{1w} = \int dkk^2\zeta_l(k)\,\hat{a}_{lm}^{1w}(k), \tag{10}$$

where $\hat{a}_{lm}^{1w}(k)$ are basis operators, which create a free massive pion with isospin component w and orbital angular momentum (l,m), and $\zeta_l(k)$ is the variational function. Working in the configuration space [9], the pion field function is defined as

$$\Phi_l = \frac{1}{2\pi}\int_0^\infty dkk^2\frac{\zeta_l(k)}{W_\pi(k)^{\frac{1}{2}}}j_l(kr). \tag{11}$$

In the following, only the $l=1$ term is used and the angular momentum label is dropped. The Fock state for the nucleon has the form [9]

$$|NT_3J_z\rangle = \Big[\alpha\big(|n\rangle\otimes\big|P_0^0\big\rangle\big)_{T_3J_z} + \beta\big(|n\rangle\otimes\big|P_1^1\big\rangle\big)_{T_3J_z} + \gamma\big(\delta\gg\otimes\big|P_1^1\big\rangle_{T_3J_z}\big)|0\rangle\Big]\Big|\sum\Big\rangle, \tag{12}$$

where $|\sum\rangle$ is the coherent σ field state with the property: $\langle\sum|\hat{\sigma}(r)|\sum\rangle = \hat{\sigma}(r)$, and $|P^{00}\rangle(|P_{1m}^{1w}\rangle)$ are the pion coherent-pair states to be determined. The normalization of the nucleon state requires the condition $\alpha^2+\beta^2+\gamma^2 = 1$. The permutation symmetric form of the $SU(2)\times SU(2)\times SU(2)$ quark wave functions imply that the source terms in the pion field equations will induce an angular momentum isospin correlation for the pion field. One can construct a coherent-pair

state with the quantum numbers of the vacuum from $l = 1$ partial waves in the following form:

$$\left|P_0^0\right\rangle = \sum \frac{f_n}{2n!}\left[b_1^{1\dagger} : b_1^{1\dagger}\right]|0\rangle\,, \tag{13}$$

where the double-dot notation refers to spin-isospin. Hence we can define the coherence parameter x with the following form:

$$b_1^{1\dagger} : b_1^{1\dagger}\,|P\rangle = x\,|P\rangle, \tag{14}$$

where $|P\rangle$ can be either $|P_0^0\rangle$ or $|P_1^1\rangle$. The x is the eigenvalue of the eigenstates $|P_0^0\rangle$ or $|P_1^1\rangle$ of a scalar operator $b_1^{1\dagger} : b_1^{1\dagger}$. The coherence parameter is related to the angular momentum l by the relation $x = (2l + 1)ab$ where a and b are coefficients that were calculated in a previous work [9].

Equation (12) allows us to calculate the expectation value of π^4 and therefore the Fock state of the pion should have components involving the excitations of many bosons, one pion, two pions, excitations that are coupled to the proper angular momentum (l) and isospin quantum number (w). The coherence parameter x relates the pionic contributions of the observables. In the following section, we show that equations of motion depend on the coherence parameter x as well as the observables of the nucleon (for details, see Ref. [8]).

IV. VARIATIONAL PRINCIPLE

The objective of this section is to seek a minimum of the total baryon energy, which is given by

$$E_N = \langle NT_3J_z|\int_0^\infty d^3r : H(r) : |NT_3J_z\rangle. \tag{15}$$

The field equations are obtained by minimizing the total energy of the nucleon with respect to the variation of the fields, $\{u(r), v(r), \sigma(r), \Phi(r)\}$, as well as the Fock-space parameters, $\{\alpha, \beta, \gamma\}$, subjected to the normalization conditions. The total energy of the system is written as

$$E_N = 4\pi\int_0^\infty dr r^2 \varepsilon_N(r)\,. \tag{16}$$

Writing the quark Dirac spinor as

$$\Psi_{\frac{1}{2}m}^{\frac{1}{2}w}(\mathbf{r}) = \begin{pmatrix} u(r) \\ v(r)\,\sigma\cdot\hat{\mathbf{r}} \end{pmatrix}\chi_{\frac{1}{2}m}\zeta^{\frac{1}{2}w}, \tag{17}$$

the energy density is given by

$$\begin{aligned}
\varepsilon_N(r) = {} & \frac{1}{2}\left(\frac{d\sigma}{dr}\right)^2 + \frac{\lambda^2}{4}[\sigma^2(r) - v^2]^2 - m_\pi^2 f_\pi \sigma(r) \\
& + 3\left\{u(r)\left(\frac{dv}{dr} + \frac{2}{r}v(r)\right) - v(r)\frac{du}{dr}\right. \\
& \left. + g\sigma(r)[u^2(r) - v^2(r)]\right\} + (N_\pi + x) \\
& \times\left(\left(\frac{d\Phi}{dr}\right)^2 + \frac{2}{r^2}\Phi^2(r)\right) + (N_\pi - x)\,\Phi_p^2(r) \\
& - \alpha\delta g(a+b)\,u(r)\,v(r)\,\Phi(r) + \lambda^2\{x^2 + 2xN_\pi \\
& + 81[\alpha^2a^2c^2 + (\beta^2+\gamma^2)d^2]\}\Phi^4(r) \\
& + \lambda^2(N_\pi + x)[\sigma^2(r) - v^2]\Phi^2(r) \\
& - \frac{\pi^2}{45}T^4 + \frac{T^2}{24f_\pi^2}\left(3m_\sigma^2 - 5m_\pi^2\right)\hat{\sigma}^2 \\
& + \frac{T^2}{12f_\pi^2}\left(3m_\sigma^2 - 5m_\pi^2\right)\Phi(r)^2(N_\pi + x)
\end{aligned} \tag{18}$$

where N_π is the average pion number

$$N_\pi = 9(\alpha^2a^2 + (\beta^2+\gamma^2)c^2), \tag{19}$$

and δ takes the following values for the nucleon quantum numbers:

$$\delta_N = (5\beta + 4\sqrt{2}\gamma)/\sqrt{3}. \tag{20}$$

The function $\Phi_p(r)$ is obtained from $\Phi(r)$ by double folding

$$\Phi_p(r) = \int_0^\infty w(r,\acute{r})\,\Phi(\mathbf{r})\,r^2 d\acute{r}, \tag{21}$$

$$w(r,\acute{r}) = \frac{2}{\pi}\int_0^\infty dk k^2 w(k)\,j_1(kr)\,j_1(kr'). \tag{22}$$

For fixed α, β, and γ, the stationary functional variations are expressed by

$$\delta\left(\int_0^\infty dr r^2\{\varepsilon_N(r) - 3\epsilon[u^2(r) + v^2(r)] - 2k\Phi\Phi_p(r)\}\right) = 0, \tag{23}$$

where the parameter k enforces the pion normalization condition,

$$8\pi\int_0^\infty \Phi(r)\,\Phi_p(r)\,r^2 dr = 1, \tag{24}$$

and ϵ fixes the quark normalization,

$$4\pi\int_0^\infty [u^2(r) + v^2(r)]r^2 dr = 1. \tag{25}$$

Minimizing the Hamiltonian yields the four nonlinear coupled differential equations,

$$\frac{du}{dr} = -2(g\sigma + \epsilon)v(r) - \frac{1}{3}\alpha\delta(a+b)\,g\Phi(r)\,u(r)\,, \tag{26}$$

$$\begin{aligned}
\frac{dv}{dr} = {} & -\frac{2}{r}v(r) - 2(g\sigma(r) - \epsilon)u(r) \\
& + \frac{1}{3}\alpha\delta(a+b)\,g\Phi(r)\,u(r)\,,
\end{aligned} \tag{27}$$

$$\begin{aligned}
\frac{d^2\sigma}{dr^2} = {} & -\frac{2}{r}\frac{d\sigma}{dr} - m_\pi^2 f_\pi + 3g[u^2(r) - v^2(r)] \\
& + \lambda^2(N_\pi + x)[\sigma^2(r) - v^2]\Phi^2(r)\,\sigma(r) \\
& + \lambda^2[\sigma^2(r) - v^2]\sigma(r) + \frac{T^2}{12f_\pi^2}\left(3m_\sigma^2 - 5m_\pi^2\right)\hat{\sigma}\,,
\end{aligned} \tag{28}$$

$$\frac{d^2\Phi}{dr^2} = -\frac{2}{r}\frac{d\Phi}{dr} + \frac{2}{r^2}\Phi(r) + \frac{1}{2}\left(1 - \frac{x}{N_\pi}\right)m_\pi^2\Phi^2 + \frac{\lambda^2}{2}\left(1 + \frac{x}{N_\pi}\right)[\sigma^2(r) - v^2]\Phi(r) - \frac{\alpha}{N_\pi}(a+b)\,g\delta u(r)v(r) + \frac{\lambda^2}{N_\pi}\{x^2 + 2xN_\pi + 81[\alpha^2a^2c^2 + (\beta^2+\gamma^2)d^2]\}\Phi^3(r) - \frac{k}{N_\pi}\Phi_p(r) + \frac{T^2}{24f_\pi^2}\left(3m_\sigma^2 - 5m_\pi^2\right)\Phi(r)\left(1 + \frac{x}{N_\pi}\right), \tag{29}$$

with the eigenvalues ϵ and k. The above equations consist of two quark equations for u and v where $\sigma(r)$ and $\Phi(r)$ appear as potentials and two Klein-Gordon equations with $u(r)v(r)$ and $[(u^2(r) - v^2(r)]$ are source terms. The coefficients a, b, and c are functions in the coherence parameter x and the field equations are solved for the fixed coherence parameter x and the fixed Fock-space parameters (α, β, γ) as in Ref. [9].

V. NUCLEON PROPERTIES

The expectation value of the energy is minimized with respect to (α, β, γ) by diagonalizing the energy matrix

$$\begin{bmatrix} H_{\alpha\alpha} & H_{\alpha\beta} & H_{\alpha\gamma} \\ H_{\alpha\beta} & H_{\beta\beta} & H_{\beta\gamma} \\ H_{\alpha\gamma} & H_{\beta\gamma} & H_{\gamma\gamma} \end{bmatrix} \begin{bmatrix} \alpha \\ \beta \\ \gamma \end{bmatrix} = E \begin{bmatrix} \alpha \\ \beta \\ \gamma \end{bmatrix}, \tag{30}$$

where each H entry of the matrix is related to a corresponding density as follows:

$$H_{\alpha\beta} = 4\pi \int r^2 E_{\alpha\beta}(r)dr, \tag{31}$$

with similar definitions for the other entries. The functions for a nucleon are

$$E_{\alpha\alpha} = E_0(r) + 18a^2\Phi_P^2 + 9a^2\lambda^2(2x + 9c^2)\Phi^4(r) + 9\lambda^2a^2[\sigma^2(r) - v^2]\Phi^2(r) + \frac{T^2}{12f_\pi^2}\left(3m_\sigma^2 - 5m_\pi^2\right)\Phi^2(r)a^2, \tag{32}$$

$$E_{\beta\beta} = E_0(r) + 18c^2\Phi_P^2 + 9\lambda^2(2xc^2 + 9d^2)\Phi^4(r) + 9\lambda^2c^2[\sigma^2(r) - v^2]\Phi^2(r) + \frac{T^2}{12f_\pi^2}\left(3m_\sigma^2 - 5m_\pi^2\right)\Phi^2(r)c^2, \tag{33}$$

$$E_{\gamma\gamma} = E_0(r) + 18c^2\Phi_P^2 + 9\lambda^2(2xc^2 + 9d^2)\Phi^4(r) + 9\lambda^2c^2[\sigma^2(r) - v^2]\Phi^2(r) + \frac{T^2}{12f_\pi^2}\left(3m_\sigma^2 - 5m_\pi^2\right)\Phi^2(r)c^2, \tag{34}$$

$$E_{\alpha\beta} = -2g(a+b)\Phi(r)u(r)v(r)\frac{2\sqrt{2}}{\sqrt{3}}, \tag{35}$$

$$E_{\alpha\gamma} = -2g(a+b)\Phi(r)u(r)v(r)\frac{5}{\sqrt{3}}, \tag{36}$$

where

$$E_0(r) = \frac{1}{2}\left(\frac{d\sigma}{dr}\right)^2 + \lambda^2x^2\Phi^4(r) + 3g\sigma(r)[u^2(r) - v^2(r)] - m_\pi^2 f_\pi\sigma(r) + 3\left\{u(r)\left[\frac{dv}{dr} + \frac{2}{r}v(r) - v(r)\right]\frac{du}{dr}\right\} + \frac{\lambda^2}{4}[\sigma^2(r) - v^2]^2 + \lambda^2x[\sigma^2(r) - v^2]\Phi^2(r) - \frac{\pi^2}{45}T^4 + \frac{T^2}{24f_\pi^2}\left(3m_\sigma^2 - 5m_\pi^2\right)[2x\Phi^2(r) + \sigma^2] - \lambda^2m_\pi^2\Phi^2(r) - U_0, \tag{37}$$

where U_0 is the minimum of potential U at $(\sigma = f_\pi, \pi = 0)$.

A. Mass of the nucleon

In this subsection, we calculate the total energy of the nucleon, which consists of quark, σ, pion, quark-σ interaction, quark-pion interaction, and meson static energy contributions. The nucleon mass was derived as in Ref. [9]

$$(K.E)_{\text{quark}} = \int_0^\infty [g\sigma\rho_s(r) + \epsilon\rho_w(r) + g\pi\rho_p(r)]r^2dr, \tag{38}$$

where ρ_s, ρ_p, and ρ_w are the quark scalar density, pseudoscalar density, and vector density, respectively. Similarly, one can find the meson kinetic contribution

$$(K.E.)_{\text{sigma}} = \frac{1}{2}\int_0^\infty \sigma(r)\Big(-m_\pi^2 f_\pi + 3g(u^2(r) - v^2(r)) + \lambda^2(N_\pi + x)(\sigma^2(r) - v^2)\Phi^2(r)\sigma(r) + \lambda^2(\sigma^2(r) - v^2)\sigma(r) + \frac{T^2}{12f_\pi^2}\left(3m_\sigma^2 - 5m_\pi^2\right)\hat{\sigma}\Big)r^2dr \tag{39}$$

$$(K.E.)_{\text{pion}} = \frac{1}{2}\int_0^\infty \Phi(r)\left(\frac{2}{r^2}\Phi(r) + \frac{1}{2}\left(1 - \frac{x}{N_\pi}\right)m_\pi^2\Phi^2 + \frac{\lambda^2}{2}\left(1 + \frac{x}{N_\pi}\right)(\sigma^2(r) - v^2)\Phi(r) - \frac{\alpha}{4N_\pi}(a+b)\,g\delta u(r)v(r) + \frac{\lambda^2}{N_\pi}[x^2 + 2xN_\pi + 81(\alpha^2a^2c^2 + (\beta^2+\gamma^2)d^2)]\Phi^3(r) - \frac{k}{N_\pi}\Phi_p(r) + \frac{T^2}{24f_\pi^2}\left(3m_\sigma^2 - 5m_\pi^2\right)\Phi(r) \times \left(1 + \frac{x}{N_\pi}\right)\right)r^2dr. \tag{40}$$

The quark-meson interaction energy takes the form

$$E_{\text{q-sigma}} = -\int_0^\infty g\sigma\rho_s(r)r^2dr \tag{41}$$

$$E_{\text{q-pion}} = -\int_0^\infty g\sigma\rho_p(r)r^2dr, \tag{42}$$

and the meson-meson interaction energy is

$$E_{\text{meson-meson}} = \int_0^\infty \left(\frac{\lambda^2}{4}(\hat{\sigma}^2 + \hat{\pi}^2 - v^2)^2 - f_\pi m_\pi^2 \hat{\sigma} - \frac{\pi^2}{45}T^4 + \frac{T^2}{24 f_\pi^2}\left(3m_\sigma^2 - 5m_\pi^2\right)(\hat{\sigma}^2 + \hat{\pi}^2) + U_0 \right) r^2 dr. \quad (43)$$

B. Magnetic moment, axial-vector coupling constant ($\frac{g_A}{g_v}$), and pion-nucleon coupling constant $g_{\pi NN}(0)$

From the electromagnetic current operator [9]

$$j^\mu_{\text{em}} = \overline{\Psi}\left(\tfrac{1}{6} + \tfrac{1}{2}\tau_3\right)\Psi + \epsilon_{3\alpha\beta}\phi_a \partial^\mu \phi_\beta, \quad (44)$$

one can derive the magnetic moments of the proton and the neutron

$$\frac{\mu_p(r)}{4\pi e} = \frac{ruv}{81}(54\alpha^2 + 2\beta^2 + \gamma^2 + 32\sqrt{2}\beta\gamma) + \frac{x}{729a^2}(9a^2 + x)(4\beta^2 + \gamma^2)\Phi^2, \quad (45)$$

$$\frac{\mu_n(r)}{4\pi e} = \frac{ruv}{81}(-36\alpha^2 - 8\beta^2 + \gamma^2 - 32\sqrt{2}\beta\gamma) - \frac{x}{729a^2}(9a^2 + x)(4\beta^2 + \gamma^2)\Phi^2. \quad (46)$$

The axial-vector coupling constant, measured in neutron β decay, is a matrix element of the space part of the isovector-axial vector current. Specifically, one is interested in $\frac{g_A}{g_v}$, where g_v is the corresponding matrix element of the isovector-vector current

$$\mathbf{J}^V_\mu = \tfrac{1}{2}\overline{\Psi}\gamma^\mu\hat{\Psi} + \hat{\pi} \times \partial^\mu \hat{\pi}. \quad (47)$$

The values of g_A and g_v are taken from the z component in space and the third component in isospace. Since the vector part yields $\frac{1}{2}$, one obtains [9]

$$\frac{g_A}{g_v} = 4\pi \int_0^\infty dr r^2 \left[\left(\frac{5}{3}\alpha^2 + \frac{5}{27}\beta^2 + \frac{25}{27}\gamma^2 + \frac{32\sqrt{2}}{27}\beta\gamma \right) \times \left(u^2(r) - \frac{v^2(r)}{3} \right) + \frac{8}{3\sqrt{3}}\alpha\beta(a+b)\frac{d\sigma}{dr}\Phi \right]. \quad (48)$$

The change in the magnetic moments, and coupling constant ($\frac{g_A}{g_v}$) is induced by the dynamics of the fields in Eqs. (26)–(29). At $T = 0$, the field equations are recovered as in Ref. [9].

VI. RESULTS AND DISCUSSION

In the present approach, the nucleon appears as a self-consistent localized stationary solution (soliton) in a suitable modified Gell-Levy σ model using a variational procedure with a spin and isospin projection [9]. In this model, the SU(2)×SU(2) chiral symmetry corresponds to the real world of one σ and three pions. We use the values at zero temperature as the initial conditions of the numerical calculation. The initial parameters are determined from the condition at $T = 0$. The mass of the σ particle in the data group ranges from 400 to 1200 MeV [36]. We took $m_\sigma = 450$ MeV as a typical value. The set of equations of motion has been solved in the same iterative manner as in Ref. [9]. The iteration procedure is implemented as follows. For fixed values of x, α, β, and γ, the above differential equations with the corresponding boundary conditions are solved by using the modified numerical package COLSYS code. This process is repeated until self-consistency is achieved.

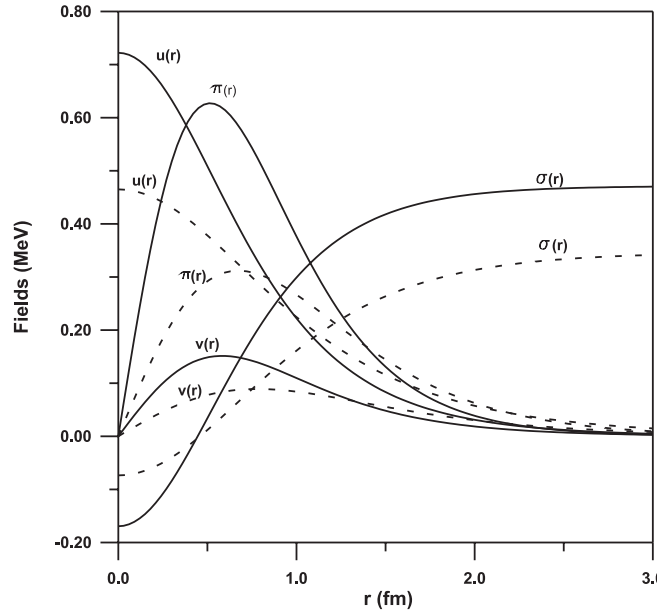

FIG. 1. σ, pion, and the components $[u(r), v(r)]$ of the quark fields are plotted as functions of the radial distance r, where the continuous curves are for $T = 0$ and the dashed curves are for $T = 100$ MeV.

A. Nucleon properties

In this subsection, we examine the nucleon observables under the effect of finite temperature. First, we examine the dependence of the quark components $u(r), v(r)$, σ field and pion fields on the temperature. In Fig. 1, we have plotted the above fields as functions of the radial distance r at zero and finite temperature ($T = 100$ MeV), respectively. At finite temperature, the σ field starts at $\sigma = -0.07$ MeV and starts increasing with increasing radial distance r. The pion field $\pi(r)$ has a P-wave form. It reaches its maximum at $r = 0.57$ fm and then it decreases until it reaches again a zero value. The function $u(r)$ equals 0.46 MeV at $r = 0$ and then it decreases until it reaches zero as $r \to \infty$. The function $v(r)$ takes the same behavior as the pion field. We note that the behavior is similar in the two cases where the fields are shifted to lower values compared to the zero-temperature case. Hence the finite temperature will have an effect on the mesonic and quark contributions and therefore on the nucleon properties as will be explained in the next paragraph.

In Fig. 2, the nucleon mass is plotted as a function of the temperature. One can see that the nucleon mass monotonically increases with increasing temperature and slightly decreases at higher values of the temperature. The behavior is in agreement

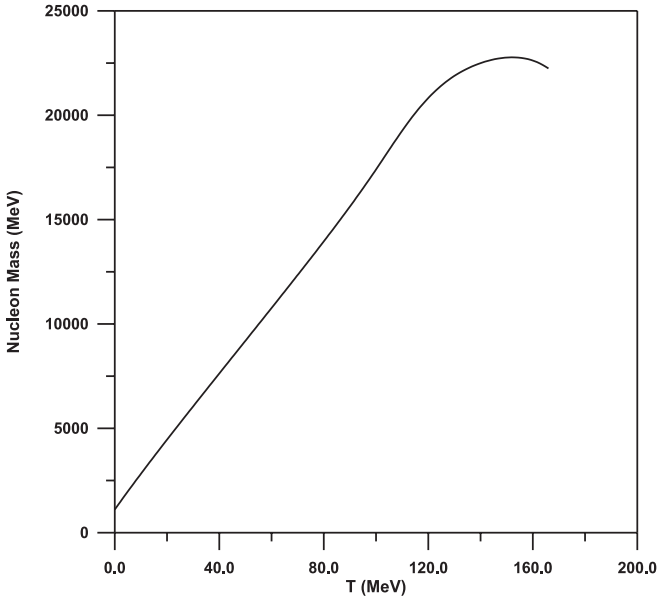

FIG. 2. The nucleon mass is plotted as a function of the temperature T.

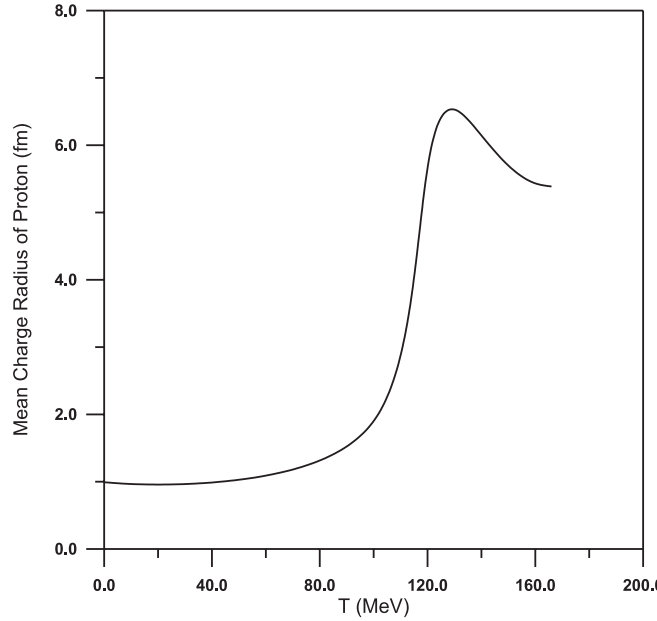

FIG. 3. The mean charge radius of the proton is plotted as a function of the temperature T.

with Christov *et al*. [30]. They noticed that the nucleon mass increases until a value of $\frac{3}{4}T_c$ (T_c is critical temperature). In the present work, the critical temperature is taken as $T_c = \sqrt{3}f_\pi \simeq$ 161MeV, which is in agreement with Ref. [35]. Bernard and Meissner [37] deduced a similar behavior with the Skyrme model with vector mesons. Berger and Christov [38] noticed that the nucleon mass increases with increasing temperature for different densities using the Nambu-Jona-Lasinio model up to 150 MeV. In addition, Dominguez and Loewe [39] deduced that the nucleon mass increases with increasing temperature. They studied the nucleon propagator at finite temperature in the framework of finite energy QCD sum rules. They also interpreted their results as a phase deconfinement transition. Our present work is in agreement with the Dominguez and Loewe [39] calculation. In contrast, Zokaut [33] obtained a nucleon mass that decreases with increasing temperature. In his work, the nucleon mass is calculated by using the Bethe-Salpeter equation where the nucleon is considered as a scalar-diquark and a quark, in which the interaction between the diquark and the quark is taken as an exchange of a quark. In Fig. 3, we note that the mean-square radius of the proton changes slightly with increasing temperature T up to 80 MeV and sharply increases in the range from 80 MeV to 120 MeV and then slightly decreases at higher values of the temperature near the critical point temperature. Dominguez *et al*. [32] obtained the radius of the nucleon, which increases as T increases. This was interpreted as deconfinement of the nucleon mass. A similar conclusion can be drawn in the present work. In Fig. 4, we note that the mean-square radius of the neutron changes slightly at lower values of the temperature below 158 MeV and then starts increasing sharply at higher temperature values near the critical point temperature.

In Fig. 5, the proton and neutron magnetic moments are calculated as functions of the temperature. The proton and neutron magnetic moments have the same picture as the nucleon mass, that is, they increase with temperature up to 0.76 T_c then sharply decrease at higher temperature values. This behavior is in agreement with Ref. [30]. At zero temperature, we note that the values of the proton and neutron magnetic moments $\mu_p = 2.0$ and $\mu_n = -1.75$ for initial parameters $m_\sigma = 450$ MeV, $g = 4.5$ are in agreement with Ref. [9]. Figures 6 and 7 show the behavior of the quantities for $g_A(0)$ and $g_{\pi NN}$ (0) as a function of T. The behavior of $g_{\pi NN}$ (0) is in agreement with Dominguez *et al*. [32] and Dey *et al*. [40]. They found that $g_{\pi NN}$ decreases

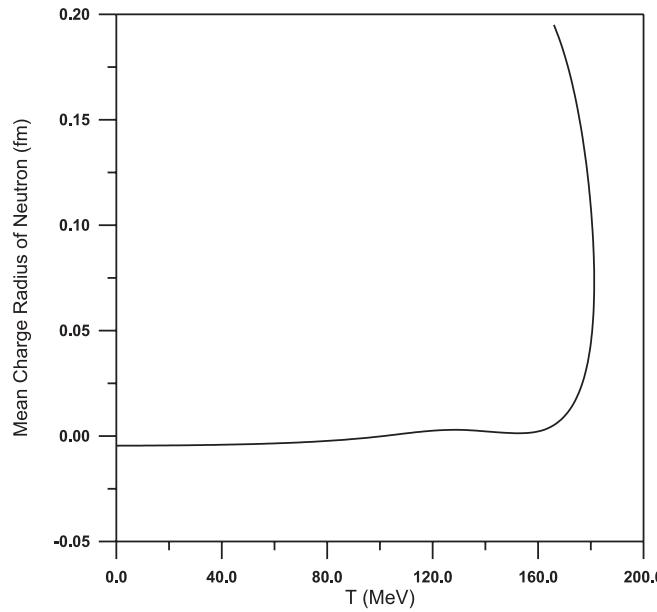

FIG. 4. The mean charge radius of the neutron is plotted as a function of the temperature T.

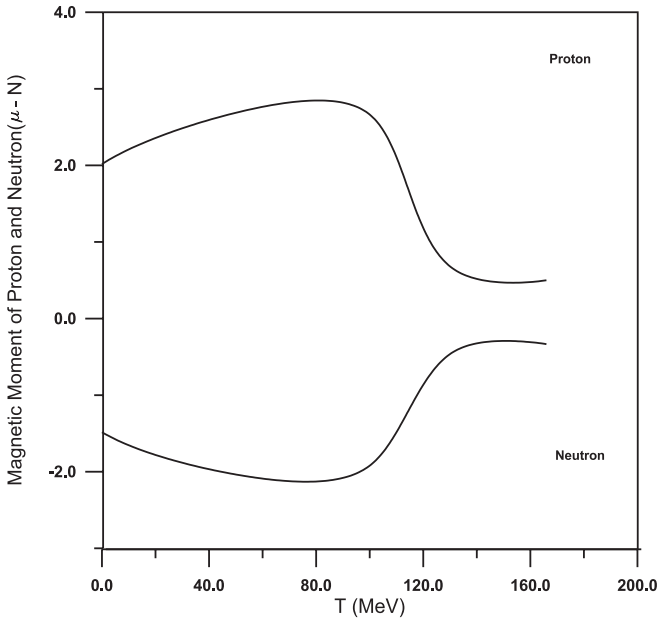

FIG. 5. The magnetic moments of a proton and a neutron are plotted as a function of the temperature T.

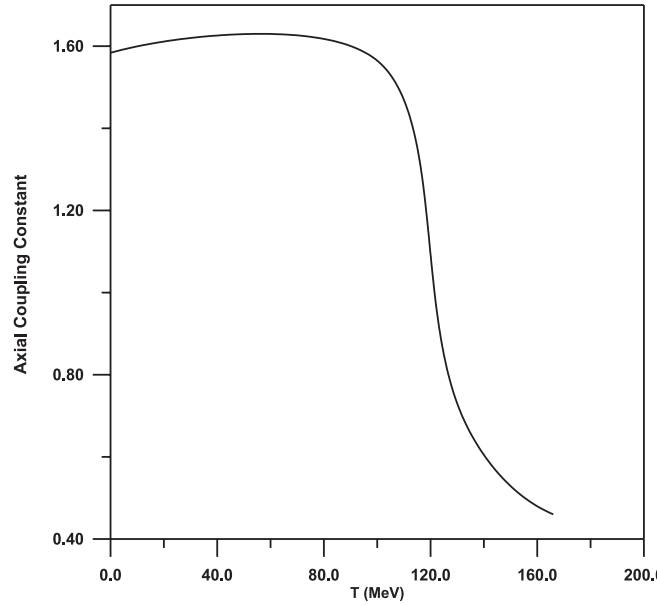

FIG. 7. The axial coupling constant is plotted as a function of temperature T.

at higher values of the temperature. In the present work, we find that the nucleon mass and mean-square radius of proton increases as a function of the temperature, whereas the pion-nucleon coupling constant decreases at higher temperature values, which is interpreted as a deconfinement phase [32]. In Ref. [41], the authors found that the σ-nucleon coupling constant obtains $g_{NN\sigma}(0) = \frac{g_q^\sigma}{g_q^\pi} g_{NN\pi}(0)$ where g_q^σ and g_q^π are quark-σ coupling and quark-pion coupling, respectively. In the linear σ model, where the g_q^σ and g_q^π are equal then the behavior of the σ-nucleon coupling constant takes the same behavior of the pion-nucleon coupling constant in Fig. 6, showing the deconfinement phase transition is satisfied with respect to $g_{NN\sigma}(0)$ at higher values of the temperature.

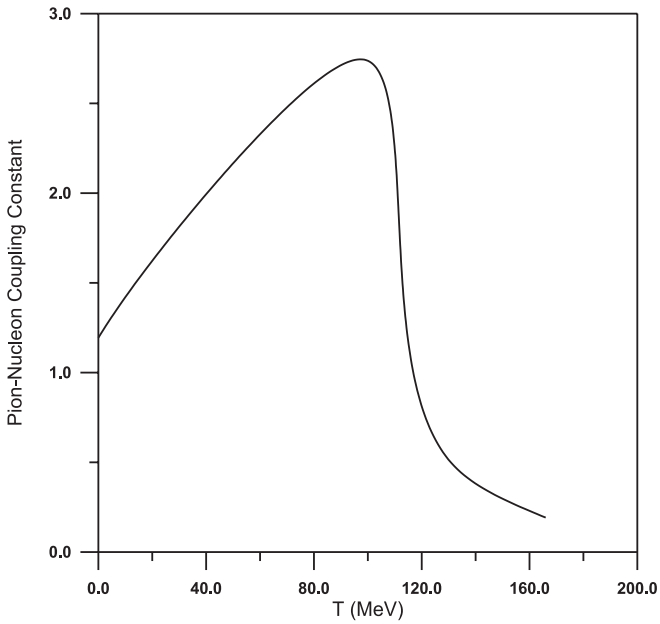

FIG. 6. The pion-nucleon coupling constant is plotted as a function of the temperature T.

It is important to examine the effect of the coherence parameter x on the nucleon properties at finite temperature and the reason why the results are sensitive to it. In Sec. II, we note that the coherence parameter x is related to the pionic contributions. This means that any increase in the coherence parameter x will lead to an increase in the mesonic contributions to the nucleon properties (see Table I). Table I shows that the nucleon properties are sensitive to the change of the coherence parameter x. The mesonic contributions are sensitively affected by changing the coherence parameter x at the critical point temperature where the mean-square radius of the proton is increased by about 15%. Also, the mean-square radius of the neutron is observed to strongly change from a negative value to a positive value. We note that the mesonic contributions in the charge radius of the proton and neutron increase when the coherence parameter x is increased. A similar situation is found for the magnetic moment of the proton and neutron, in which the mesonic contributions increase with increasing parameter x. In addition, the $g_A(0)$ values are reduced by about 23% with increasing x. The $g_{\pi NN}(0)$ strongly decreases with increasing x, since the coupling constant is weakened by the increase of x. In Figs. 8 and 9, we examined the nucleon mass and mean-square radius of the proton in the (T, x) plane, where the T axis is taken in units of f_π to be dimensionless, as is the coherence parameter x. In Fig. 8, we plotted the nucleon mass as a function of x and T, and we note that the surface increases as both T and x increase. In Fig. 9, the similar behavior is shown for the mean-square radius of the proton, which slightly increases up to $(T, x) \simeq (0.6, 1.2)$ and then sharply increases with increasing coherence parameter x. Figures show that by increasing the coherence parameter, the nucleon mass and the

TABLE I. The observables of the nucleon calculated for two values of coherence parameter, $x = 0.3$ and $x = 3$ at $T_c = 161$ MeV, $m_\sigma = 450$ MeV, and $g = 4.5$.

x		$x = 0.3$			$x = 3$	
Quantity	Quark	Meson	Total	Quark	Meson	Total
$\langle r^2\rangle_p$	3.937	-2.370×10^{-5}	3.937	4.655	4.75×10^{-3}	4.660
$\langle r^2\rangle_n$	-6.171×10^{-5}	2.370×10^{-5}	-3.8×10^{-5}	6.77×10^{-3}	-4.753×10^{-3}	2.01×10^{-3}
μ_p	2.4928	1.099×10^{-5}	2.492	1.541	1.358×10^{-2}	1.555
μ_n	-1.661	-1.099×10^{-5}	-1.661	-1.031	-1.358×10^{-2}	-1.0445
$g_A(0)$	0.631	1.377×10^{-5}	0.631	0.4696	1.448×10^{-2}	0.484
$g_{\pi NN}$	1.3898	7.6×10^{-4}	1.390	0.864	-0.105	0.7596

mean-square radius of the proton values increase in a faster way at higher temperature values.

VII. SUMMARY AND CONCLUSION

It is interesting to compare the nucleon Fock state in the present approach with those used in other works. In Refs. [8,9], the authors calculated the nucleon properties at zero temperature where the mesonic potential was used in the zero-order loop. This order is sufficient for calculating the nucleon properties at zero temperature. Moreover, the coherence parameter was fixed to the value $x = 1$, since the increase of the coherence parameter x will increase the pionic contributions, leading to an increase in the energy of nucleon mass, which conflicts with the data. In the present work, we extended the work of Ref. [9] by introducing the effective mesonic potential at one loop to include the effect of finite temperature on the nucleon properties. Chiku and Hatsuda [29] examined the optimal perturbation theory (OPT) at finite temperature in the linear σ model, in which the loopwise expansion in (OPT) is shown to be a suitable scheme to resume higher-order terms. They did not examine the nucleon properties such as the nucleon mass and mean-square radius of proton in their work. Dominguez *et al.* [32] calculated the pion-nucleon constant and mean square radius of the proton as functions of the temperature. Thermal fluctuations are only considered and they ignored quantum fluctuations in their model. They found that the pion-nucleon constant and the mean-square radius of the proton increase with increasing temperature; therefore they interpreted it to be a deconfinement phase transition. In the present work, we find that the nucleon mass and mean-radius of the proton increase with temperature, hence the deconfinement is satisfied in the present work. Also, Dominguez and Loewe [39] studied the nucleon propagator at finite temperature in the framework of finite energy QCD sum rules. They found that the nucleon mass increases with increasing temperature T. This result is in agreement with our result, which indicates the deconfinement phase. In Refs. [29,32,39], the authors did not calculate the magnetic moment of the proton and neutron and also did not consider the quantization of the fields. Caldas *et al.* [34] calculated the fermion mass and they found that it increases

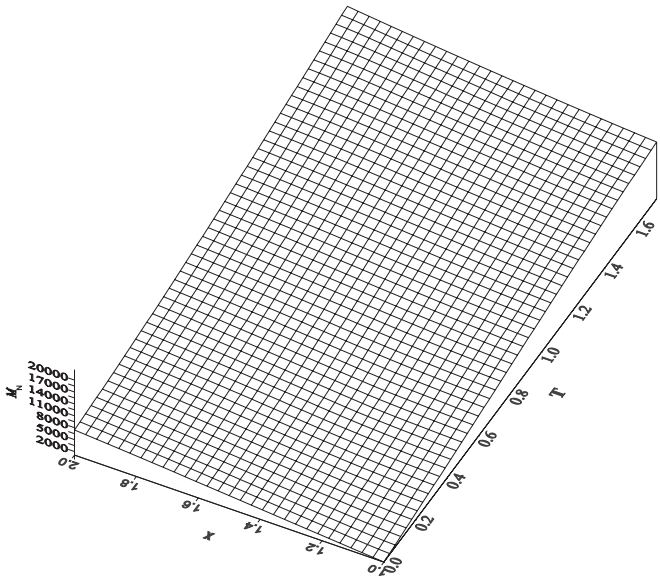

FIG. 8. The nucleon mass dependance on the coherence parameter x and the temperature T. The T is in units of f_π, where the T and x are in dimensionless units and the nucleon mass is in MeV.

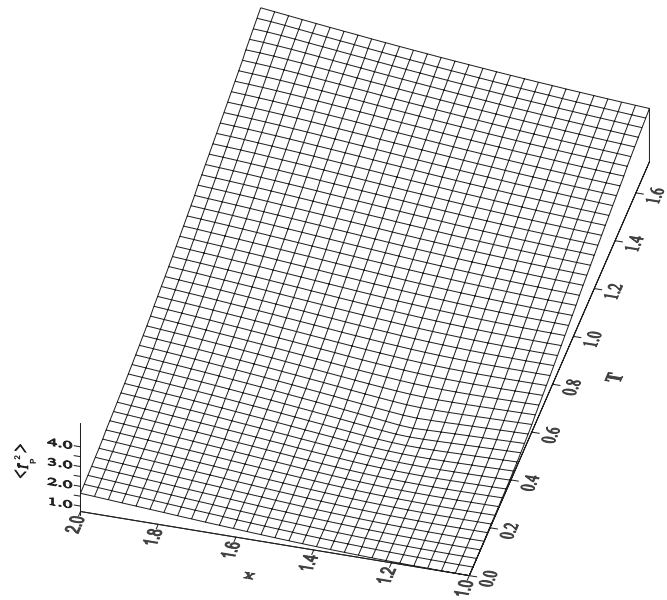

FIG. 9. The radius of the proton dependance on the coherence parameter x and the temperature T. The T is in units of f_π, where the T and x are in dimensionless units and the mean-square radius of proton is in fm.

with increasing temperature, which is in agreement with the present result. Caldas *et al*. [34] did not calculate other nucleon properties such as nucleon magnetic moments and the coupling constant. Also, the quantization of fields is not considered in their model. To conclude, we have investigated nucleon properties such as the nucleon mass, mean-square radius of the proton and neutron, coupling constant g_A, and pion-nucleon coupling constant $g_{\pi NN}$ as functions of the temperature T using the linear σ model. We quantized the meson and quark fields in the Hamiltonian density and then minimized the Hamiltonian density to get the field equations. The field equations have been solved by an iteration method using modified COLSYS code. We found that the nucleon mass and the mean-square radius of the proton and the neutron increase with increasing temperature, and the pion-nucleon coupling constant decreases sharply near the critical temperature. Also, we examined the nucleon mass and mean-square radius of the proton in the (T, x) plane. The results obtained are comparable with other approaches and indicate a deconfinement phase transition.

[1] G. A. Contrera, D. G. Dumm, and N. N. Scoccola, XI HADRON PHYSICS **1296**, 326 (2010).
[2] D. H. Rischke, Prog. Part. Nucl. Phys. **52**, 197 (2004).
[3] *Proceedings of Quark Matter'93*, edited by E. Stenlund, H. A. Gustafsson, A. Oskarsson, and I. Otterlund, Nucl. Phys. A **566**, 449 (1994).
[4] V. S. Timoteo and C. L. Lima, Phys. Lett. B **635**, 168 (2006).
[5] M. Gell-Mann and M. Levy, Nuovo Cinmento **24**, 705 (1960).
[6] M. C. Birse and M. K. Banerjee, Phys. Rev. D **31**, 118 (1985).
[7] B. Golli and M. Rosina, Phys. Lett. B **165**, 347 (1985).
[8] K. Goeke, M. Harvey, F. Grummer, and J. N. Urbano, Phys. Rev. D **37**, 754 (1988).
[9] T. Ali, J. A. McNeil, and S. Pruess, Phys. Rev. D **60**, 114022 (1999).
[10] W. Broniowski and B. Golli, Nucl. Phys. A **714**, 575 (2003).
[11] M. Rashdan, M. Abu-Shady, and T. S. T. Ali, Int. J. Mod. Phys. E **15**, 143 (2006).
[12] M. Rashdan, M. Abu-Shady, and T. S. T. Ali, Int. J. Mod. Phys. A **22**, 2673 (2007).
[13] M. Abu-Shady, Mod. Phys. Lett. A. **24**, 20 (2009).
[14] M. Abu-Shady and M. Rashdan, Phys. Rev. C **81**, 015203 (2010).
[15] M. Abu-Shady, Inter. J. Mod. Phys. A **26**, 235 (2011).
[16] G. Amelina-Camelia and S. Y. Pi, Phys. Rev. D **47**, 2356 (1993).
[17] G. Amelino-Camelia, Phys. Lett. B **407**, 268 (1997).
[18] H. Verschelde and J. D. Pessemier, Eur. Phys. J. C **22**, 771 (2002).
[19] N. Pertropoulos, J. Phys. G **25**, 2225 (1999).
[20] J. T. Lenaghan, D. H. Rischke, and J. Schaffner-Bielich, Phys. Rev. D **62**, 085008 (2000).
[21] D. Roder, J. Ruppert, and D. H. Rischke, Phys. Rev. D **68**, 016003 (2003).
[22] Y. Nemoto, K. Naito, and M. Oka, Eur. Phys. J. A **9**, 245 (2000).
[23] J. Baacke and S. Michalski, Phys. Rev. D **67**, 085006 (2003).
[24] J. M. Cornwall, R. Jackiw, and E. Tomboulis, Phys. Rev. D **10**, 2428 (1974).
[25] S. Shu and J.-R. Li, J. Phys. G **31**, 459 (2005).
[26] H. Mao, N. Petropoulos, S. Shu, and W. Zhao, J. Phys. G **32**, 2187 (2006).
[27] O. Scavenius, A. Mocsy, I. N. Mishustin, and D. H. Rischke, Phys. Rev. C **64**, 045202 (2001).
[28] J. T. Lenaghan and D. H. Rischke, J. Phys. G **26**, 431 (2002).
[29] S. Chiku and T. Hatsuda, Phys. Rev. D **58**, 076001 (1998).
[30] C. V. Christov, E. R. Arriola, and K. Goeke, Nucl. Phys. A **556**, 641 (1993).
[31] M. Abu-Shady, Int. J. Theor. Phys. **50**, 1372 (2011).
[32] C. A. Dominguez, C. V. Gend, and M. Loewe, Nucl. Phys. B, Proc. Suppl. **86**, 413 (2000).
[33] I. Zakout (2005), arXiv:nucl-th/0502003.
[34] H. C. G. Caldas, A. L. Mota, and M. C. Nemes, Phys. Rev. D **63**, 056011 (2001).
[35] A. Das, *Finite Temperature Field Theory* (World Scientific, Singapore, 1997).
[36] P. D. Group, Eur. Phys. J. C **3**, 1 (1998).
[37] V. Bernard and U. G. Meissner, Phys. Lett. B **227**, 465 (1989).
[38] J. Berger and C. V. Christov, Nucl. Phys. A **609**, 537 (1996).
[39] C. A. Dominguez and M. Loewe, Eur. Phys. J. C **58**, 273 (1993).
[40] J. Dey, M. Dey, and P. Ghose, Phys. Lett. B **165**, 181 (1985).
[41] G. Erkol, R. G. Timmermans, and T. A. Rijken, Phys. Rev. C **72**, 035209 (2005).